Research paper

On the azimuth angle characteristics of the blast wave from an underground magazine model (VI) —The effect of the ratio between the internal diameters of the magazine chamber and passageway—

Yuta Sugiyama*†, Kunihiko Wakabayashi*, Tomoharu Matsumura*, and Yoshio Nakayama*

*National Institute of Advanced Industrial Science and Technology (AIST), Central 5, 1−1−1 Higashi, Tsukuba-shi, Ibaraki, 305−8565 JAPAN
Phone: +81−29−861−0552
†Corresponding author: yuta.sugiyama@aist.go.jp

Received: June 14, 2019 Accepted: December 9, 2019

Abstract

Small-scale explosion experiments were conducted to assess the effect of the shape of a modeled underground magazine on the outside blast-wave propagation. The magazine model was divided into a chamber and a passageway; the internal diameter of the chamber (D_0) was fixed at 38.8 mm, while that of the passageway (D_1) was varied so that their ratio (D_1/D_0) ranged at 0.26 and 0.76. The results were compared with the experimental ones previously reported for $D_1/D_0 = 0.51$ and 1.00. The experiments provided the azimuthal distribution of the peak overpressure for this model, showing that a narrow passageway can greatly mitigate the peak overpressure outside the magazine under the tested conditions. The data were obtained to determine the isobar of the peak overpressure for an arbitrary shaped underground magazine. An empirical equation of this experimental isobar is proposed for a circumscribed circle; the properties of the center and radius of this circle were described as a linear function of the scaled radius of the isobar of the surface explosion and their gradients decreased when reducing D_1/D_0.

Keywords: scale-model experiment, overpressure distribution, high explosive, magazine shape effect, hazardous materials management.

1. Introduction

In industrial activities, local and instantaneous high pressure can be utilized for mining and blasting excavation; in addition, high explosives are often used because their detonation rapidly releases a large amount of energy. However, an accidental initiation can generate a blast wave, causing a physical hazard to humans and structures whose severity is determined by blast parameters such as peak overpressure and positive impulse. The peak overpressure is an instantaneous and maximum value, while the positive impulse is calculated as the time integral of the positive overpressure between the first incident blast wave being recorded and the overpressure returning to zero. The extent of the damage caused depends on the distance between the magazine where the explosives are stored and a working/residential area[1]. The safety distance is known as the explosive safety quantity distance (ESQD). To properly estimate the physical hazard from the blast-wave strength and ensure the safe commercial applications and storage of high explosives, the blast-wave characteristics must be investigated; such measurements could allow appropriate standards for the storage of high explosives in magazines.

High explosives are stored in many different types of magazines. Explosions in aboveground magazines can be considered as surface explosions of the hemispherical high explosives on the ground; the isobar of the peak overpressure, required for estimating the ESQD, could be described as a circle whose center corresponds with that of the hemispherical high explosives since the hemispherical blast wave expands from it[2]. In such cases, the ESQD is independent of the azimuth angle. During

explosions in underground magazines[3)–6)] for storing the high explosive are partially confined, on the other hand, the blast wave propagates inside the magazines after initiation and exits from the opening. Previous studies[7)–9)] have demonstrated that the blast-wave strength outside the magazine is determined by the exit characteristic length and the peak overpressure at the exit and depends on azimuth angle. Since the blast wave exits via one end of the magazine, the peak overpressure is greatest along the exit direction. Unlike in a surface explosion, this strength and, hence, also the ESQD depend on the azimuth angle from the exit. Therefore, the blast-wave propagation outside the magazine should be understood to define safety regulations taking the azimuth angle into account.

We performed a series of tests including small-scale explosion experiments[10)–12)], numerical simulations[13)], and field experiments[14)] to investigate the effect of the magazine shape on the blast-wave strength and azimuthal distribution. In our previous works[10), 11)], we considered underground magazines shaped like a simple tube, whose cross-sectional area was constant over the whole length, and experimentally evaluated the effect of the ratio between the internal diameter (D) and the magazine length (L), L/D.

However, in real situations, a typical underground magazine can be divided into a storage chamber and a passageway for carrying the explosives to and from this chamber. Therefore, we investigated the effect of the ratio between the inner lengths of the chamber (L_0) and passageway (L_1) (i.e., L_1/L_0)[12)], which ranged between 0.125 and 2.0 when the ratio of the corresponding internal diameters (D_1/D_0) was 0.51; L_1/L_0 did not influence the peak overpressures and isobars outside the magazine, but narrowing the passageway mitigated the blast-wave strength for the considered D_1/D_0.

The previous work showed that D_1/D_0 is an important parameter to discuss the blast-wave strength. In the present study, to estimate the peak overpressure distribution in the case of an arbitrary shaped underground magazine, we conducted additional tests to understand the effect of D_1/D_0 on the blast-wave characteristics.

2. Experimental details

2.1 Test explosive

The test explosive was the same as in our previous studies[10)–12)] and its details are reported in Sugiyama et al.[10)] Two 0.50 g pressed pellets of pentaerythritol tetranitrate (PETN, 95 wt %) and carbon powder (5 wt %) were glued together to be used as a 1.00 g explosive charge; an electrical detonator with 0.1 g of lead azide was glued to one end of the pellet.

2.2 Experimental setup

The experimental setup was as in the previous tests[10)–12)]. Since the Japanese regulation of underground magazines (Article 25 of Ordinance for Enforcement of the Explosive Control Act) requires a protective dike near the exit to minimize the damage caused by the blast waves and fragments, we included a dike model in our tests. Figure 1 shows a schematic of the magazine, cover, exit, and dike models mounted on a steel plate; L_0 and L_1 were fixed at 310.4 and 38.8 mm, respectively, while D_0 and D_1 were varied. Table 1 summarizes the parameter values used in the present (labeled as D_1/D_0 = 0.76 and 0.26) and previous (labeled as D_1/D_0 = 1.00[11)] and 0.51[12)]) tests. Since we did not divide the underground magazine into two sections (namely, chamber and passageway) in one of these previous experiments[11)], we interpreted the corresponding D_0 and D_1 as identical and equal to 38.8 mm, resulting in the label D_1/D_0 = 1.00 in Table 1.

The present study differed from our previous tests[11), 12)] also in terms of dike size. It was designed with reference

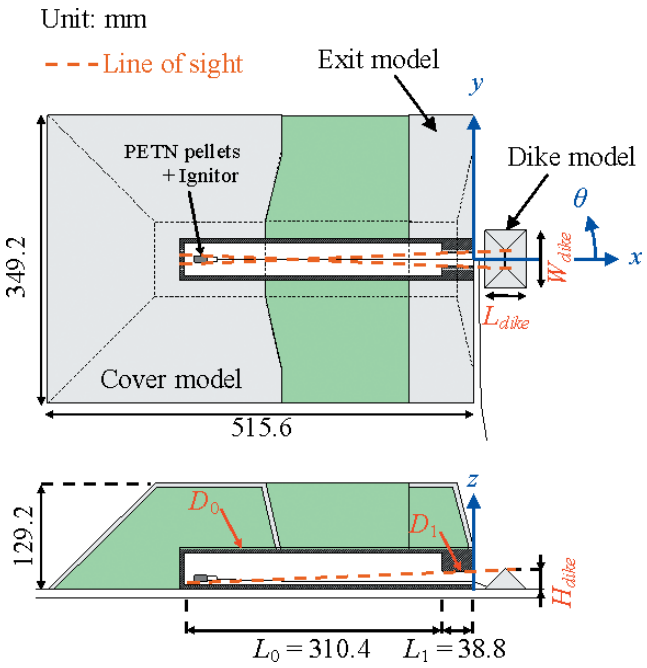

Figure 1 Schematic (top and side views) of the magazine and dike models. D_0 and D_1 denote the internal diameters of the chamber and passageway, respectively, and L_0 and L_1 indicate the corresponding internal lengths. L_{dike}, W_{dike}, and H_{dike} denote the length, width, and height of the dike. The diameters were varied. The brown dashed lines represent the line of sight not to see through the high explosive charge inside the chamber from the outside to determine the dike size.

Table 1 Table 1 Values of the parameters used in the present and previous tests[11), 12)].

D_0 [mm]	D_1 [mm]	D_1/D_0	L_{dike} [mm]	W_{dike} [mm]	H_{dike} [mm]
38.8	38.8	1.00[11)]	123.0	202.0	60.0
	29.3	0.76	80.4	113.6	38.7
	19.9	0.51[12)]	58.4	79.0	27.7
	9.9	0.26	36.8	45.7	16.9

to the line of sight not to see through the high explosive charge inside the chamber from the outside (brown dashed line in Figure 1). In the present case, the dike was large enough to obscure the line of sight; its length (L_{dike}), width (W_{dike}), and height (H_{dike}) are also listed in Table 1. D_1 increment enlarged the dike size.

The magazine model was constructed using a cylindrical steel pipe and the height of the cover model was 129.2 mm. We expected the occurrence of complex blast-wave reflections around the exit and dike models, and therefore a solid wall was required near the exit to maintain the exit shape and ensure the repeatability of the measurements; this exit wall was made of steel. We filled the space between the exit and the cover models with clay having a density of 2230 kg m^{-3}. Since the acoustic impedance of clay is much larger than that of air, any energy absorbed from the air could be neglected.

The center of the explosive charge was placed 20 mm from the end wall of the cylindrical steel pipe. The origin of the (x, y, z) coordinate system was set on the steel plate at the exit and the azimuth angle was defined as increasing counterclockwise from the x-axis. The upper surface of the steel plate was defined as the ground surface in the experiments and located at xy surface (z=0) as shown in Figure 1.

In addition, we conducted surface explosion experiments without any magazine model to observe the strength of an unimpeded blast wave. In this case, the explosive was placed vertically to generate a two-dimensional axisymmetric blast wave; the height between its center and the steel plate was 18 mm.

2.3 Measurements

The blast-wave pressures were measured using piezoelectric pressure sensors (PCB 113B28, 14.5 mV kPa^{-1}) and a digital waveform recorder (H-TECH Triple Mode 30622). The sensors were installed on the steel plate, at different distances from the magazine exit (400, 800, 1200, and 1600 mm) which were the same conditions as we reported previously[10)–12)]. Since the magazine model is symmetric with respect to the zx plane, the sensors were placed at azimuth intervals of 10° between 0° and 180°. The sensor at 400 mm from the exit and azimuth angle between 160° and 180° was under the magazine model; therefore, we did not record the pressure-time histories at these points.

Explosion tests were conducted to verify the reproducibility of the peak overpressure distribution and to determine how the azimuth angle affects the blast wave emerging from the magazine exit. The values were averaged over two or three trials. After these experiments, no deformation of the model, made of steel, was observed.

3. Results and discussion

For the safety analysis, we focused on the peak overpressures. To discuss the azimuth angle characteristics of the blast wave, the experimental pressure-time histories were used to obtain the peak overpressures. Here, the azimuth angle characteristics are defined as how the peak overpressure is attenuated by increasing the azimuth angle at each radius between magazine exit and pressure sensors. The data of both this study and the previous papers[10)–12),14)] are expressed in terms of distance scaled to the cube root of mass of the explosive (R, in m $kg^{-1/3}$): in the current experiments, 1 m $kg^{-1/3}$ corresponds to 100 mm since the estimated energy released by the detonator was about 2 % that of the PETN pellets[15)] and, hence, negligible to calculate the scaled distance. We used the following scaled coordinate system:

$$X = \frac{x}{m^{1/3}},\ Y = \frac{y}{m^{1/3}},\ R = \sqrt{X^2+Y^2}, \tag{1}$$

where m is the mass of the explosive (in this case, 1.00 g). The corresponding R values were 4, 8, 12, and 16 m $kg^{-1/3}$ for the various pressure sensor locations.

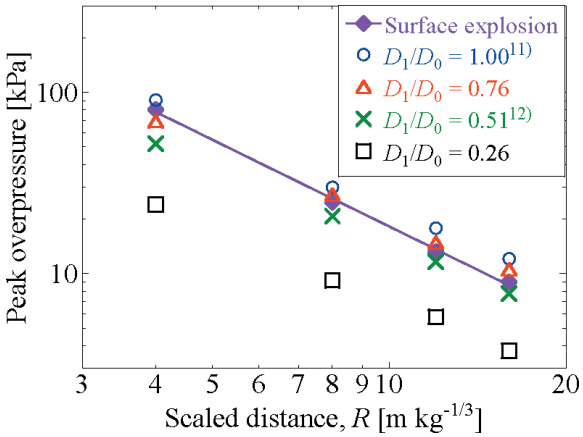

Figure 2 The peak overpressure distribution at 0° for both explosions inside the underground magazine and surface explosion. In the case of the surface explosion, the solid line is described by Equation 2.

Figure 2 shows the peak overpressure distribution at 0° for both explosions inside the underground magazine and surface explosions. The empirical equation of peak overpressure $p_{surface}$ for surface explosions, used to discuss the isobar of the peak overpressures of the underground magazine, can be written as

$$\log(p_{surface}) = -1.59 \log R + 2.85. \tag{2}$$

As regards the explosions in the magazine at 0°, decreasing D_1/D_0 reduced their peak overpressures, which were always smaller than those of the surface explosion for $D_1/D_0 \leq 0.51$. Therefore, the internal diameter ratio is an important factor to discuss the blast-wave strength from underground magazines and could be used to determine the ESQD.

In Figure 2, the linear attenuation ratio of the peak overpressures, which denotes their decrement by volumetric expansion of the blast wave, is almost the same in all cases. Although the formation mechanisms of the blast waves for the two types of explosion were different, hemispherical volumetric expansion occurred in both; thus, the linear attenuation ratio was not much dependent on the experimental conditions. As regards the blast-wave generation, in the surface explosions, it occurred by the

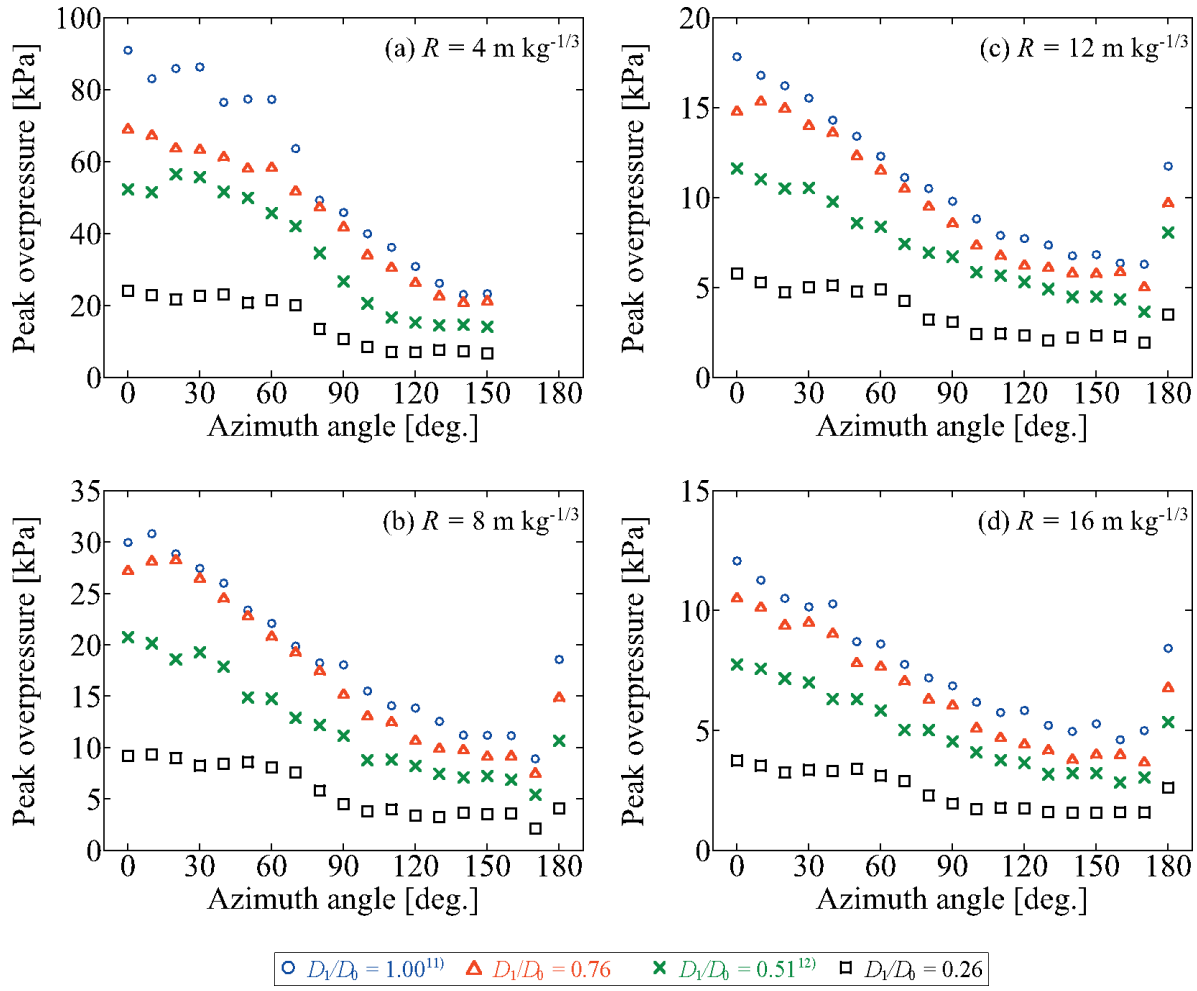

Figure 3 Azimuthal distribution of the peak overpressures, measured by pressure sensors at different observation points (R).

initiation of the PETN pellets and, hence, its strength was strongly dependent on the distance from the explosive. On the other hand, in the explosions inside the magazine, the blast wave was released from the exit. Thus, physical parameters such as peak overpressure at the exit and the exit geometry are important factors to determine the blast -wave strength. In the present study, the difference in the peak overpressure distributions for the underground magazine was caused by the different D_1 values tested.

Figure 3 shows the azimuthal distributions of the peak overpressures for various observation points. The azimuth angle increment resulted in decreased peak overpressure, except at around 180°, where it increased locally. Given the symmetrical and angular shape of the cover model, as shown in Figure 1, the blast waves propagating behind it from the $+y$, $-y$, and $+z$ directions were strengthened by their coupling[10)–14)]. As the passageway became narrower, the peak overpressures were much mitigated. Table 2 lists the normalized and angle-averaged peak overpressures. The data in Figure 3 are normalized with respect to those of D_1/D_0 = 1.00 for each scaled distance, and the points obtained between 0° and 180° are averaged for each scaled distance. The averaged values are listed in four columns, where "Average" denotes the averaged values of the four scaled distances above and is defined as P. The normalized peak overpressures were independent of the scaled distance.

Table 2 The normalized and angle-averaged peak overpressures.

Scaled distance [m kg$^{-1/3}$]	D_1/D_0 = 0.76	D_1/D_0 = 0.51[12)]	D_1/D_0 = 0.26
4	0.83	0.60	0.27
8	0.89	0.64	0.30
12	0.88	0.67	0.33
16	0.85	0.65	0.32
Average, (defined as P)	0.87	0.64	0.30

In a previous study[14)], we proposed a conversion factor from the peak overpressure ratio (vertical axis data) to the distance ratio (horizontal axis data) in the peak overpressure distribution. Here, we applied the same idea as follows. The linear attenuation ratio of the peak overpressures for the surface explosion in Equation 2 was estimated as −1.59. Given the log-log plots, the conversion factor for the radius (f_r) was estimated based on the peak overpressure ratio (P) values reported in Table 2 and this estimated linear attenuation ratio: $f_r = (1/\mathrm{P})^{-1/1.59}$. It denotes the distance ratio normalized with respect to distance in the case of D_1/D_0 = 1.00, where the same peak overpressure was obtained for every D_1/D_0. The conversion factor for the radius were calculated as 0.916,

Table 3 Values of the fitting parameters l and m calculated using Equation 3 for D_1/D_0 = 0.76 and 0.26 at various azimuth angles (θ).

θ [°]	D_1/D_0 = 0.76		D_1/D_0 = 0.26	
	l	m	l	m
0	−1.372	2.667	−1.325	2.174
10	−1.366	2.663	−1.348	2.177
20	−1.375	2.655	−1.379	2.175
30	−1.376	2.642	−1.371	2.174
40	−1.381	2.626	−1.389	2.196
50	−1.442	2.644	−1.319	2.115
60	−1.465	2.647	−1.379	2.162
70	−1.443	2.585	−1.405	2.150
80	−1.457	2.556	−1.293	1.914
90	−1.404	2.462	−1.200	1.752
100	−1.376	2.361	−1.144	1.615
110	−1.361	2.313	−0.998	1.466
120	−1.294	2.201	−0.997	1.441
130	−1.214	2.092	−1.140	1.558
140	−1.219	2.071	−1.110	1.543
150	−1.198	2.051	−1.034	1.464
160	−1.195	2.050	−1.177	1.622
170	−1.027	1.809	−0.404	0.701
180	−1.127	2.196	−0.639	1.203

0.755, and 0.469 for D_1/D_0 = 0.76, 0.51, and 0.26, respectively. The D_1/D_0 reduction greatly decreased the distance ratio, showing that the ESQD was strongly related to D_1/D_0.

To calculate the peak overpressure distribution outside the underground magazine, the correlations between the peak overpressures p_{peak} and scaled distances R for each experimental condition were fitted with log-log plots. The fitting parameters l and m were obtained as follows:

$$\log(p_{peak}) = l \log R + m. \quad (3)$$

Table 3 lists their values estimated for D_1/D_0 = 0.76 and 0.26 for the present study; those at D_1/D_0 = 1.00 and 0.51 have already been calculated by Sugiyama et al.[11),12)].

Now, let's discuss the peak overpressure distribution around the magazine exit to understand the physics of the blast-wave expansion. Figure 4 schematizes the changes in the isobars of the peak overpressures caused by the two types of explosion considered in this study. In surface explosions (i.e., in aboveground magazines), as already explained, these isobars can be described as circles whose center corresponds with that of the hemispherical high explosives and not dependent on the azimuth angle, as shown in Figure 4a. In contrast, for explosions inside an underground magazine, the azimuthal distribution of the peak overpressures changes the shape of their isobars depending on the angle. In this case, we assume that the origin is located at the exit and the isobars are still described as circles, but their center moves in the $+x$ direction. Figure 4 and the following equation describe the geometrical conversion from the isobars of a surface explosion into those of an explosion from an underground

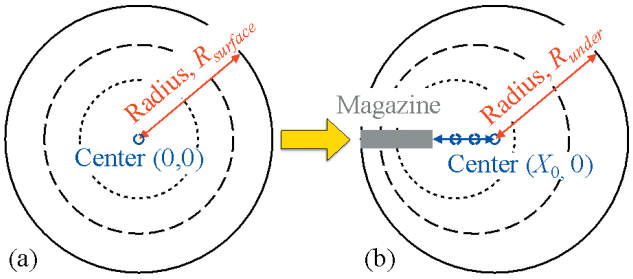

Figure 4 Changes in the isobar of the peak overpressure caused by (a) a surface explosion and (b) an explosion inside an underground magazine.

magazine:

$$X^2 + Y^2 = R_{surface}^2 \rightarrow (X - X_0)^2 + Y^2 = R_{under}^2. \quad (4)$$

$R_{surface}$, and R_{under} denote the scaled radii of the isobar for the surface explosion and an explosion from an underground magazine, and X_0 denotes the scaled center location in X-axis. The following assumptions were made to obtain the circle described in Equation 4.

1. The circumscribed circles with the minimum radius are obtained from the experimental isobars.
2. The parameters describing the circle (X_0 and R_{under}) are written as functions of $R_{surface}$ to facilitate the isobar comparison.
3. X_0 and R_{under} are obtained from the isobar of the surface explosion at different $R_{surface}$ (4, 8, 12, and 16 m kg$^{-1/3}$), as shown in Figure 2.
4. The effect of the cover model around 180° is negligible.

Figure 5 shows the isobars of the peak overpressures on the ground. Near the dike model, the blast-wave diffraction off the dike mitigated its strength around 0°. The space between the dike and the cover was narrow and the gas flow from the cylindrical tube was deflected from the $+X$ direction to the $\pm Y$ one. Thus, the locally strong blast wave along the $\pm Y$ direction increased the distance between the exit and the isobar, resulting in the longest distance at $X = X_0$, as shown by the dashed line in Figure 5a. Therefore, the isobar assumed an elliptical shape and circumscribed circle did not agree with the experimental isobar; this circle overestimated the exit-isobar distance, especially near the $\pm X$-axis. On the other hand, after the blast wave expanded far from the exit, the isobar became circular (Figure 5b) and the circumscribed circle could properly describe its shape. The difference in the isobar shape was determined by the initial condition of the blast-wave generation from the exit.

To discuss the properties of the circumscribed circle, Figure 6 shows the relationships of its center and radius with the radius of the surface explosion, as shown also in Figure 4; they both followed linear functions. Here, approximate lines of the experimental data were described with the following assumptions. The relationship between the isobars of the two types of explosion and their simple conversion by linear functions were demonstrated, and Table 4 shows the relationships for $R_{under}/R_{surface}$ and $X_0/R_{surface}$ in Figure 6.

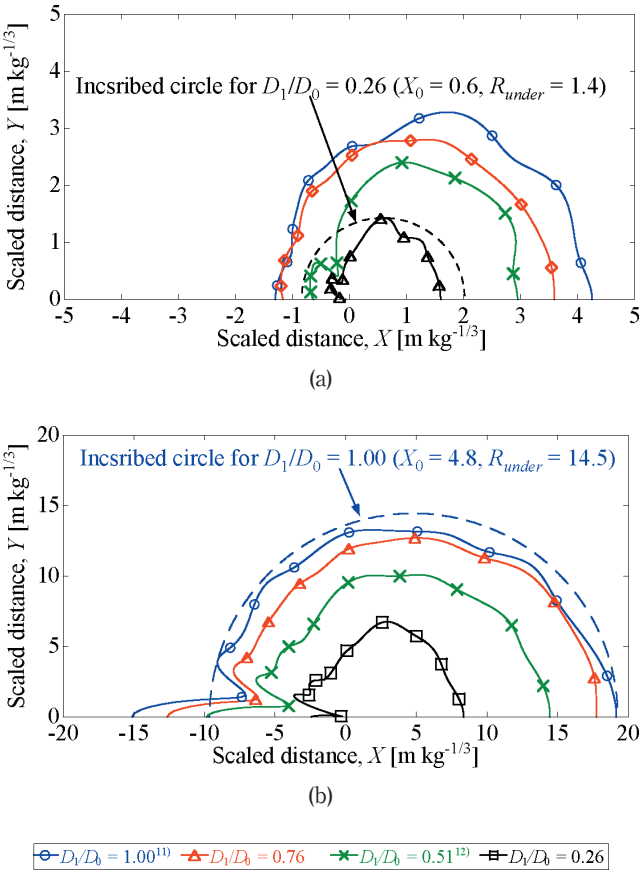

Figure 5 Isobars of the ground peak overpressures, corresponding to those of the surface explosion experiments at scaled distances of (a) 4 m kg$^{-1/3}$ and (b) 16 m kg$^{-1/3}$ shown in Figure 2. The origin is located at the magazine exit.

Table 4 Relationships for $R_{under}/R_{surface}$ and $X_0/R_{surface}$ in Figure 6.

D_1/D_0	$R_{under}/R_{surface}$	$X_0/R_{surface}$
1.00	0.91428	0.31250
0.76	0.82857	0.29786
0.51	0.66500	0.25000
0.26	0.43000	0.18286

1. The gradient of each line is minimum when all experimental data are always plotted under the approximate line.
2. In Figure 6, all the approximate lines passed through the origin, which represents the starting point of the volumetric expansion of the blast wave.

The D_1/D_0 reduction mitigated the blast-wave strength, resulting in smaller isobar size (Figure 5) and smaller gradient of the approximate line (Figure 6 and Table 4). Figure 7 shows the relationship between D_1/D_0 and the normalized gradients of the approximate lines a and c (for R_{under} and X_0, respectively). The normalized gradients of the approximate lines were normalized with respect to 0.91428 and 0.31250, as shown for D_1/D_0 = 1.00 in Table 4. The red cross symbols in Figure 7 represent the f_r values estimated from the P ones listed in Table 2 and a linear attenuation ratio of −1.59 for the surface explosion shown in Figure 2. Solid lines in Figure 7 are the approximate line as

$$a = 1.1038\left(\frac{D_1}{D_0}\right)^{0.6293} - 0.1038\left(\frac{D_1}{D_0}\right)^{6.6934}, \quad (5)$$

$$c = 1.1253\left(\frac{D_1}{D_0}\right)^{0.4867} - 0.1253\left(\frac{D_1}{D_0}\right)^{4.3701}, \quad (6)$$

Here, approximate lines in Figure 7 are proposed with the following assumptions.

1. The D_1/D_0 increment increases a and c which becomes unity at D_1/D_0 = 1.00, and their gradients become zero to achieve the maximum value at D_1/D_0 = 1.00.
2. If the exit diameter (i.e., D_1) is zero, the blast wave cannot propagate outside. Therefore, a and c at D_1/D_0 = 0 become zero accordingly.

In the present study, the normalized gradient of the approximate line a for the radius agreed well with f_r, showing that the isobar radius for an underground magazine could be estimated by using the f_r value derived

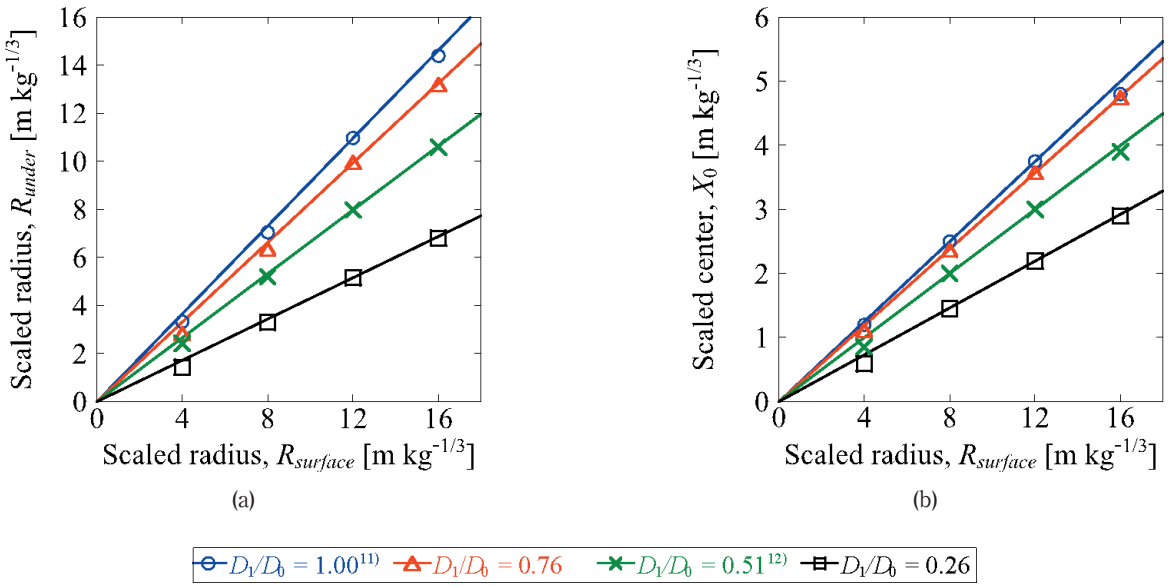

Figure 6 Relationship between the scaled radius of the surface explosion ($R_{surface}$) and (a) the scaled radius (R_{under}) and (b) scaled center (X_0) of the circumscribed circle. Approximate lines of Equations 5 and 6 were also described.

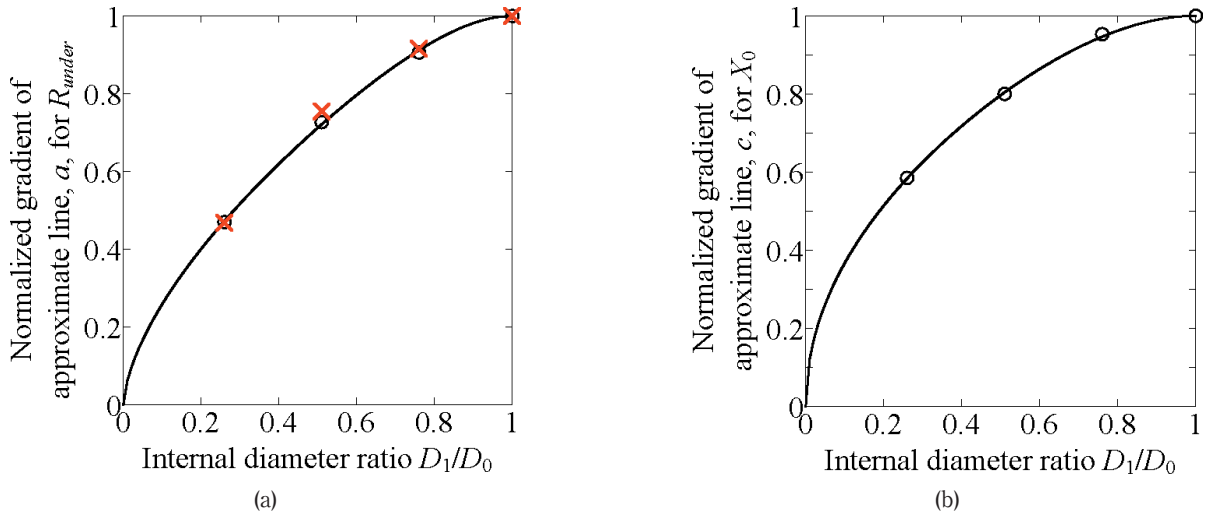

Figure 7 Relationship between the internal diameter ratio D_1/D_0 and the normalized gradients of the approximate lines (a) a and (b) c (for R_{under} and X_0, respectively, of the circumscribed circle). The red cross symbols in Figure 7a represent the f_r values.

from the linear attenuation ratio of the surface explosion (Figure 2) and the peak overpressure ratio at 0°. Since X_0 in Figure 7b is an imaginary point, it is hard to demonstrate the mechanism how X_0 is determined only by the pressure measurements and, hence, it must be still elucidated quantitatively. Therefore, for this purpose, future studies can be based also on numerical simulations.

The coupling with Equations 4, 5, and 6 and $R_{under}/R_{surface}$ = 0.91428 and $X_0/R_{surface}$ = 0.31250 as shown in the linear lines of D_1/D_0 = 1.00 of Table 4 could describe the circumscribed circle of the isobar of peak overpressures for the present underground magazine model in the case of $(L_0+L_1)/D_0$ = 9, which, in turn, could be used to determine the ESQD.

4. Conclusion

We conducted scale-model explosion experiments to determine how the presence of a narrow passageway to the storage chamber affects the azimuthal distribution of a blast wave exiting from an underground magazine. The ratio between the internal diameters of the chamber and the passageway was varied, revealing that a narrower passageway can greatly mitigate the blast-wave strength. We described the circumscribed circle of the isobars from the experimental data to discuss the blast-wave characteristics for underground magazines; its radius and center were related via linear functions to the radius of the surface explosion, demonstrating the simple linear relationship between the isobars of surface explosion and those of explosions inside the underground magazine. The experimental data allowed to obtain the isobars of peak overpressures for the present underground magazine model in the case of $(L_0+L_1)/D_0$ = 9.

Acknowledgment

This study was made possible by a Ministry of Economy, Trade, and Industry (METI) sponsored project entitled "Technical Standard for Explosion Mitigation of Explosives" in FY2018.

References

1) M. S. Mannan, "Lees' Loss Prevention in the Process Industries, 4th Edition: Hazard Identification, Assessment and Control", Butterworth-Heinemann (2012).
2) C.N. Kingery and G. Bulmash, ARBRL-TR-02555, Ballistics Research Laboratory (1984).
3) Q. Zhang, B. Qin, and D.-C. Lin, Saf. Sci., 57, 214–222, (2013).
4) D. Uystepruyst and F. Monnoyer, J. Loss Prev. Process Indust., 34, 225–231 (2015).
5) T. Abbasi and S.A. Abbasi, J. Hazard. Mater., 140, 7–44 (2007).
6) J. Taveau, J. Loss Prev. Process Indust., 23, 15–29 (2010).
7) C.N. Kingery, BRL-TR-3012, Ballistics Research Laboratory (1989).
8) C.N. Kingery and E.J. Gion, BRL-TR-3132, Ballistics Research Laboratory (1990).
9) Y. Sugiyama, K. Wakabayashi, T. Matsumura, and Y. Nakayama, Sci. Tech. Energetic Materials, 76, 14–19 (2015).
10) Y. Sugiyama, K. Wakabayashi, T. Matsumura, and Y. Nakayama, Sci. Tech. Energetic Materials, 77, 136–141 (2016).
11) Y. Sugiyama, K. Wakabayashi, T. Matsumura, and Y. Nakayama, Sci. Tech. Energetic Materials, 78, 117–123 (2017).
12) Y. Sugiyama, K. Wakabayashi, T. Matsumura, and Y. Nakayama, Sci. Tech. Energetic Materials, 80, 15–22 (2019)
13) Y. Sugiyama, K. Wakabayashi, T. Matsumura, and Y. Nakayama, Sci. Tech. Energetic Materials, 78, 49–54 (2017).
14) Y. Sugiyama, K. Wakabayashi, T. Matsumura, and Y. Nakayama, Sci. Tech. Energetic Materials, 79, 28–33 (2018).
15) M.A. Price and A.H. Ghee, Cent. Eur. J. Energetic Materials, 6, 239–254 (2009).